ASSESSMENT OF SEDIMENT ERODIBILITY OF INTERTIDAL MUDFLATS USING HYPERSPECTRAL REMOTE SENSING

S. Adam [a, *], E. Ibrahim [a], R.M. Forster [b], J. Monbaliu [a], K. Sabbe [a], E. Toorman [a], D. van der Wal [d]

[a] Hydraulics Laboratory, Katholieke Universiteit Leuven, Kasteelpark Arenberg 40, 3001 Heverlee, Belgium - (Stefanie.Adam, Elsy.Ibrahim, Jaak.Monbaliu, Erik.Toorman)@bwk.kuleuven.be
[b] Centre for Environment, Fisheries and Aquaculture Sciences, Pakefield Road, Lowestoft, Suffolk NR33 0HT, UK - r.m.forster@cefas.co.uk
[c] Laboratory for Protistology and Aquatic Ecology, Universiteit Gent, Krijgslaan 281-S8 9000 Ghent, Belgium – Koen.Sabbe@ugent.be
[d] Centre for Estuarine and Marine Ecology, Netherlands Institute of Ecology, P.O. Box 140, 4400 AC, Yerseke, The Netherlands - d.vanderwal@nioo.knaw.nl

KEY WORDS: intertidal sediment, sandbank, Molenplaat, erodibility, hyperspectral, bio-physical sediment properties

ABSTRACT:

To understand the morphodynamics of coastal regions and estuaries, accurate and detailed information on the erodibility of intertidal sediments is required as input in coastal erosion models. Sediment erodibility is dependent on bio-physical sediment properties, such as moisture and mud content, and the presence of epipelic diatoms, which is assessed by the chlorophyll *a* content.

The objective of this paper is to generate a synoptic map of sediment stability, expressed as critical shear stress, of an intertidal flat using hyperspectral remote sensing. Firstly, the potential of imaging spectroscopy to quantify mud, moisture and chlorophyll *a* content in intertidal mudflats was assessed using in situ spectral measurements and field sampling. Secondly, these models were tested and extrapolated on airborne hyperspectral data and maps of each sediment property were created. Thirdly, the results of erosion experiments performed at our and other laboratories were used to create maps of sediment stability. On the Molenplaat, an intertidal flat in the Westerschelde Estuary, The Netherlands, the critical shear stress ranged between 0.17Pa at sandy regions and 3.46Pa at muddy regions with a high density of microphytobenthos.

1. INTRODUCTION

Mudflats are important for coastal zone ecosystems by providing wildlife habitats and by acting as natural sea defences that serve to dissipate tidal and wave energy. Sediment transport and erosion models might provide information on the morphodynamic evolution of these mudflats, but require synoptic information on sediment properties, such as grain size, moisture content, the presence of macrofauna and biofilms, which can, in our regions, be quantified by chlorophyll *a*.

Deronde *et al.* (2006) classified the mud and moisture content and the amount of chlorophyll *a* using a hyperspectral airborne image and field data. The specific absorption feature of chlorophyll *a* (Méléder *et al.*, 2003; Carrère *et al.*, 2004; Combe *et al.*, 2005; Murphy *et al.*, 2005) provided interpretable results and a physically based approach to

---

* Corresponding author. Stefanie.adam@bwk.kuleuven.be

quantify the chlorophyll *a* content. Clay (Ben-dor *et al.*, 2002; Kooistra *et al.*, 2003) and moisture content (Ben-dor *et al.*, 2002) in floodplain soils and agricultural fields were quantified by wavelength selection and multivariate regression.

The objective of this paper was to create maps of mud, moisture and chlorophyll *a* content on an intertidal flat using field spectral measurements and sediment sampling, and a hyperspectral airborne image. Based on this image and the results of erosion experiments at our and other laboratories, a map showing the erodibility expressed as critical shear stress, was produced.

2. METHODS

2.1 Study Area

The Molenplaat (figure 1) is a predominantly sandy mid-channel intertidal flat in the Westerschelde estuary in the Netherlands. The surface area is approximately 1.5km^2 and the average period of emersion varies between two to four hours and up to eight hours for specific locations per tidal cycle (Herman *et al.,* 2001; Smith *et al.,* 2003).
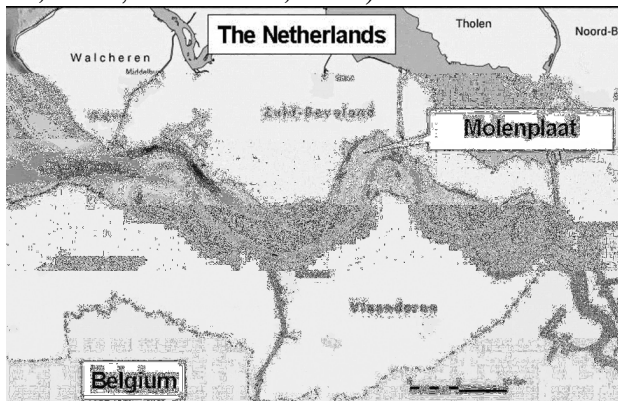

Figure 1: Location of the Molenplaat
(Deronde *et al.*, 2006)

2.2 Airborne data

On the 23rd of June 2005 at low tide conditions, an AHS (Airborne Hyperspectral Sensor) image (table 1) of the Molenplaat was acquired. The AHS system was operated by INTA on board of the CASA 212-200 aerial platform. The height of flight (1373m above ground level) was chosen so that the spatial resolution of the images was 3.4m and the swath width 2745m to cover the whole area in one flight line. The raw data were radiometrically calibrated for system errors, geometrically corrected using the PARGE software (ReSe Applications Schläpfer, Switserland), and afterwards corrected for atmospheric influences using ATCOR4 which is based on the radiometric transfer model MODTRAN 4 (Richter and Schläpfer, 2002). Simultaneously to the flight, sunphotometer measurements (with a SOLAR Microtops II) were taken to estimate the amount of water vapor and the aerosol concentration, needed for the atmospheric correction.

Module	Range (µm)	Bandwidth (nm)	Nr of bands
Visible – Near IR	0.430-1.030	30	20
Short wave IR1	1.550-1.750	200	1
Short wave IR2	1.994-2.540	13	42
Mid IR	3.300-5.400	300	7
Long wave IR	8.200-12.700	400	10

Table 1: Configuration of AHS sensor system
(IR = infrared)

2.3 Field data

Field data were collected on the 23rd of June 2005 and on the 19th of June 2007. Each sampling site was located using a GPS, and spectra were acquired with an ASD spectrometer, which records the reflectance from 350nm till 2500nm with a resolution of three nm for the region 350-1000nm and 10nm for the 1000-2500nm region. Spectral measurements were performed at a height of 0.7m with 25° field of view and nadir looking, leading to a diameter of the sampled area of ±31cm. Calibration with the Spectralon® panel was performed at least

every 30 minutes under clear sky conditions and more frequently if clouds were present. Three spectra were measured with a time interval of three seconds at each location to facilitate exclusion of erroneous measurements.

Surface sediment samples were collected with a 2.5cm diameter contact corer (Ford and Honeywill, 2002), which freezes a layer of two mm including all photosynthetically-active algal cells, as well as the bulk of sediment chlorophyll (Forster and Kromkamp, 2004). In 2005, chlorophyll *a* was extracted using 90% acetone, identified using the HPLC method by Wright *et al.* (1991) and quantified using a calibration with commercial standards. In 2007, the sediment water content was determined by calculating the weight difference after 12 hours drying at 105ºC, and mud (<64µm) content was determined in a Malvern Instruments Mastersizer2000.

2.4 Spectral analysis

The degree of absorption by chlorophyll *a* at 673nm can be characterized by i) the ratio between minimal reflectance in the absorption feature and reflectance outside the absorption feature, ii) the scaled band depth after continuum removal, and iii) the scaled band area of the absorption feature after continuum removal (Carrère *et al.*, 2004). Continuum removal is a normalization technique in order to compare absorption features from a common baseline (Clark and Roush, 1984). A regression model between these measures of the absorption feature and the sediment properties was chosen by minimizing the mean squared error of the residuals. The model parameters were estimated and the goodness of fit was expressed by the r^2 value (coefficient of determination).

The Visible and Near Infrared Analysis (VNIRA) described by Ben-dor *et al.* (2002) was applied for the selection of wavelengths to build an empirical multivariate regression to assess water and mud content. The reflectance R or derivative of the reflectance R' at wavelengths which explained the variation in a sediment property best, were selected and a linear multivariate model was built using the selected values and the field data. A multiple leave-one-out approach was used for the calibration and validation of the model, and the Root Mean Square Error (RMSE) calculated as the mean of the deviations between predicted and observed quantities of the validation data.

2.5 Erodibility map

The map showing the critical shear stress was based on i) the abiotic critical shear stress for non-cohesive sediments derived from the Shields diagram (Shields, 1936) ii) the increase in abiotic critical shear stress for cohesive sediment based on results of erosion experiments and the mud content map, iii) the increase in critical shear stress due to the presence of diatom biofilms based on results obtained by Mahatma (2004) and the chlorophyll *a* map.

3. RESULTS

3.1 Quantification of sediment properties

The relation between the ratio, scaled band depth and area of the absorption feature at 673nm and chlorophyll *a* content is a second order polynomial with $r^2 = 0.82$ for the in situ spectral measurements (n=30) and $r^2 = 0.85$ for the airborne AHS spectra (n=18) (figure 2). The relation obtained for the airborne signals was applied on the whole AHS image to create a chlorophyll *a* map.

Moisture content was significantly (p<0.001) and negatively correlated with the reflectance at all wavelengths except from 701nm till 1319nm. The best prediction potential was obtained using the reflectance at 669nm (RMSE = 2.9%, n=30 for RMC = 5.9-34.5%). This relation was applied on the AHS image to obtain a map of the moisture content.
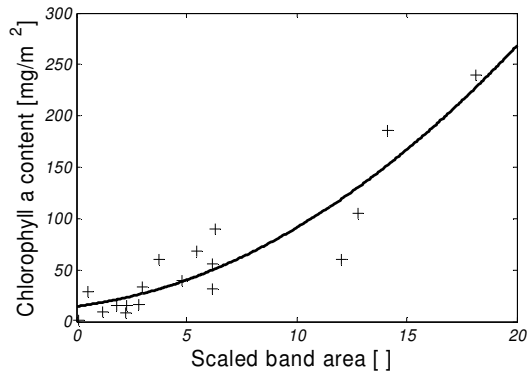
Figure 2: Relation between chlorophyll *a* content and its absorption at 673nm, measured by the AHS sensor.

For mud content, the derivative of the reflectance at 592nm and the reflectance at 673nm were retained leading to a RMSE of 8.0% (n=30, for mud = 0–46.9% by weight). This model was used to create a mud content map of the Molenplaat and a map distinguishing cohesive (>15% mud) from non-cohesive (<15% mud) sediment (figure 3).
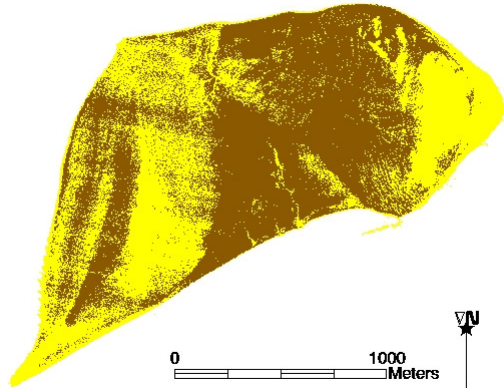

Figure 3: Sediment type map. Yellow=non-cohesive sediment, brown=cohesive sediment.

3.2 Erodibility map

The abiotic critical shear stress was determined based on the median sand diameter, the Shields diagram (Shields, 1936) and the formula of Soulsby and Whitehouse (1997), and is equal to 0.17Pa. To include the effect of cohesive sediment on the sediment stability, the critical shear stress of pixels with a mud content higher than 15% by weight, was increased according to the results

obtained in a laboratory flume and described in Adam (2009) to a value of 0.32Pa. The effect of the sediment stabilizing diatom biofilm was considered by increasing the critical shear stress with 0.0104Pa.m^2/mg (Mahatma, 2004). The final sediment stability map (figure 4) showed a critical shear stress ranging between 0.17Pa and 3.46Pa.
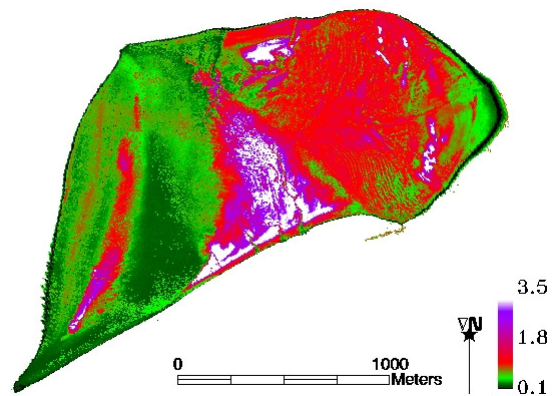

Figure 4: Map of the critical shear stress (Pa) on the Molenplaat

The moisture content of the sediment was not considered in the stability map. Moisture content has a considerable effect on the erosion rate, which is the amount of material eroded from the sediment bed (Houwing, 1999; Aberle et al., 2004). However, no clear relationship was found between moisture content and the critical shear stress in intertidal sediments (Houwing, 1999).

4. CONCLUSION

In this paper, field data, hyperspectral airborne data and experimental results were combined to obtain a map showing the sediment stability, expressed as critical shear stress, of an intertidal mudflat.

Firstly, the abiotic critical shear stress is dependent on the median sand grain diameter (Shields, 1936) and the mud content, whereby the sediment is cohesive if the mud content is > 15% by weight (Torfs, 1995; Adam, 2009). The mud fraction was estimated from the

reflectance in the red light and from the slope in the visible light. This slope was also used by Hakvoort *et al.* (1997) to discriminate between sandy and muddy sediment. The resulting map (figure 3) was very similar to the map obtained by Deronde *et al.* (2006).

Secondly, epipelic diatoms, which can be assessed by the chlorophyll *a* content, strengthen the sediment by secreting extacellular mucopolysaccharides which bind the sediment particles together (Mahatma, 2004; Riethmüller *et al.*, 2004). The chlorophyll *a* content was assessed by quantifying the absorption dip at 673nm (Carrère, 2004; Murphy, 2005) and an experimental model based on field data and image spectra. The biotic critical shear stress was calculated using the experimental results of Mahatma (2004).

Combining the abiotic and biotic critical shear stress resulted in a map showing the critical shear stress for the sediments of the Molenplaat. Whether erosion occurs, depends on the hydrodynamics of the flow and the resulting forces. This map can be used as input for sediment transport models. On the other hand, maps of sediment type of consecutive years are useful to assess the evolution on the mudflat and to verify sediment transport models.

REFERENCES

Aberle, J., Nikora, V., Walters, R., 2004. Effects of bed material properties on cohesive sediment erosion. *Marine Geology*, 207, pp. 83-93.

Adam, S., 2009. Bio-physical characterization of indicators of sediment stability of mudflats using remote sensing. PhD dissertation.

Ben-dor, E., Patkin, K., Banin, A. and Karnieli, A., 2002. Mapping of several soil properties using DAIS-7915 hyperspectral scanner data - a case study over clayey soils in Israel. *International Journal of Remote Sensing*, 23, pp. 1043-1062.

Carrère, V., Spilmont, N. and Davoult, D., 2004. Comparison of simple techniques for estimating chlorophyll *a* concentration in the intertidal zone using high spectral-resolution field-spectrometer data. *Marine Ecology Progress Series*, 274, pp. 31-40.

Clark, R.N. and Roush, T., 1984. Reflectance spectroscopy: quantitative analysis techniques for remote sensing applications. *Journal of Geophysical Research,* 89, pp. 6329-6340.

Combe, J-P., Launeau, P., Carrère, V., Despan, D., Méléder, V., Barillé, L. and Sotin, C., 2005. Mapping microphytobenthos biomass by non-linear inversion of visible-infrared hyperspectral images. *Remote Sensing of Environment*, 98, pp. 371-387.

Deronde, B., Kempeneers, P. and Forster, R.M., 2006. Imaging spectroscopy as a tool to study sediment characteristics on a tidal sandbank in the Westerschelde. *Estuarine, Coastal and Shelf Science*, 69, pp. 580-590.

Ford, R.B. and Honeywill, C., 2002. Grazing on intertidal microphytobenthos by macrofauna: is pheophorbide a useful marker? *Marine Ecology-Progress Series,* 229, pp. 33-42.

Forster, R.M. and Kromkamp, J.C., 2004. Modelling the effects of chlorophyll fluorescence from subsurface layers on photosynthetic efficiency measurements in microphytobenthic algae. *Marine Ecology Progress Series*, 284, pp. 9-22.

Hakvoort, H., Heymann, K., Stein, C. and Murphy, D., 1997. In-situ optical measurements of sediment type and phytobenthos of tidal flats: a basis for imaging remote sensing spectroscopy. *Deutsche Hydrographische Zeitschrift / German Journal of Hydrography*, 49, pp. 367-373.

Herman, P.M.J., Middelburg, J.J. and Heip, C.H.R., 2001. Review article. Benthic community structure and sediment processes on an intertidal flat: results from the ECOFLAT project. *Continental Shelf Research,* 21, pp. 2055-2071.

Houwing, E.-J., 1999. Determination of the critical erosion threshold of cohesive sediments on intertidal mudflats along the Dutch Wadden Sea Coast. *Estuarine, Coastal and Shelf Science*, 49, pp. 545-555.

Kooistra, L., Wanders, J., Epema, G.F., Leuven, R.S.B.W., Wehrens, R. and Buydens, L.M.C., 2003. The potential of field spectroscopy for the assessment of sediment properties in river floodplains. *Analytica Chimica Acta*, 484, pp. 189-200.

Mahatma, 2004. The spatial and temporal patterns of erodibility of an intertidal flat in the East Frisian Wadden Sea, Germany. PhD dissertation.

Méléder, V., Barillé, L., Launeau, P., Carrère, V. and Rincé Y., 2003. Spectrometric constraint in analysis of benthic diatom biomass using monospecific cultures. *Remote Sensing of Environment,* 88, pp. 386-400.

Murphy, R.J., Tolhurst, T.J., Chapman, M.G. and Underwood, A.J., 2005. Estimation of surface chlorophyll-*a* on an emersed mudflat using field spectrometry: accuracy of ratios and derivative-based approaches. *International Journal of Remote Sensing*, 26, pp. 1835-1859.

Richter, R. and Schläpfer, D., 2002. Geo-atmospheric processing of airborne imaging spectrometry data. Part 2, Atmospheric/Topographic Correction. *International Journal of Remote Sensing,* 23, pp. 2631-2649.

Riethmüller, R., Heineke, M., Kühl, H. and Keuker-Rüdiger, R., 2000. Chlorophyll *a* concentration as an index of sediment surface stabilisation by microphytobenthos? *Continental Shelf Research*, 20, pp. 1351-1372.

Shields, A., 1936. Application of similarity principles and turbulence research to bed-load movement. *Mitteilunger der Preussischen Versuchsanstalt für Wasserbau und Schiffbau*, 26, pp. 5-24.

Smith, G, Thomson, A., Müller, I. and Kromkamp, J., 2003. Hyperspectral imaging for mapping sediment characteristics. Presented at the 3rd workshop on Imaging Spectroscopy, Herrsching.

Soulsby, R.L. and Whitehouse, R.J.S.W., 1997. Threshold of sediment motion in coastal environments. In: *Proceedings Pacific Coasts and Ports '97*, Christchurch, New Zealand, pp. 149-154.

Torfs, H., 1995. Erosion of mud/sand mixtures. PhD dissertation.

Wright, S.W., Jeffrey, S.W., Mantoura, R.F.C., Llewellyn, C.A., Bjornland, T., Repeat, D. and Welshmeyer, N., 1991. Improved HPLC method for the analysis of chlorophylls and carotenoids from marine phytoplankton. *Marine Ecology Progress Series*, 77, pp. 183-196.